Vibrational-Energy Redistribution and Vibronic Coupling in 1-Naphthol·Water Complexes

Richard Knochenmuss,*,† Volker Karbach,† Claudia Wickleder,‡ Stephan Graf,§ and Samuel Leutwyler§

LOC, Universitätsstr. 16, ETH Zentrum, 8092 Zürich, Switzerland, Institut für Anorganische Chemie, Universität zur Köln, Greinstr. 6, 50939, Köln, Germany, and Departement für Chemie und Biochemie, Universität Bern, Freiestrasse 3, 3000 Bern 9, Switzerland

Received: June 25, 1997; In Final Form: November 24, 1997

Resonant two-photon ionization (R2PI) and fluorescence spectra of the 1-naphthol·H_2O and 1-naphthol-d_1·D_2O cluster are reported and interpreted with emphasis on intracomplex vibrational energy redistribution (IVR) and vibronic coupling. The analysis included an ab initio normal-coordinate calculation of both complexes at the 6-31G (d,p) level. In $S_1 \leftarrow S_0$ R2PI spectra, the intermolecular modes were found to be very weak; only one such S_1 vibration was observed at 57 cm^{-1} (54 cm^{-1} for 1-naphthol-OD·D_2O). At excitations less than 400 cm^{-1} above the $S_1 \leftarrow S_0$ origin, the fluorescence spectra retain a simple 1-naphthol-like pattern. At higher excess energies, the fluorescence exhibits complex structure due to emission from both relaxed and unrelaxed S_1 vibrational states, showing efficient coupling through the hydrogen bond. This restricted IVR behavior changes to dissipative IVR at about 834 cm^{-1} above the $S_1 \leftarrow S_0$ origin. Exceptions to general IVR are observed. The $S_1 + 403$ cm^{-1} level is a restricted IVR case, while the nearby $S_1 + 400$ cm^{-1} level undergoes nearly dissipative IVR. On the other hand, a nearly "frozen" mode is observed at 553 cm^{-1} above the $S_1 \leftarrow S_0$ origin. By use of the ab initio vibrational analysis and lowest-order anharmonic coupling, the IVR-active vibrational "bath" states can be predicted, enabling tentative assignment of much of the relaxed fluorescence structure. Ion-dip spectroscopy shows that IVR in the electronic ground state may have a higher onset threshold than in the S_1 by ≥ 130 cm^{-1}. Exciting one quantum of the 57 cm^{-1} intermolecular mode results in a decreased S_0 IVR threshold. The strong vibronic S_1-S_2 coupling earlier observed for vibrations at $S_1 + 410$ and $S_1 + 414$ cm^{-1} in free 1-naphthol was found to be partially inhibited in 1-naphthol·H_2O but still significant in 1-naphthol-OD·D_2O. This is attributed to harmonic mode mixing. In contrast, vibronic coupling becomes active in the $S_1 + 292$ cm^{-1} level of 1-naphthol·H_2O.

Introduction

The excited-state proton transfer (ESPT) reaction of 1-naphthol (NpOH) to water and other solvents has received considerable attention as a model for proton-transfer reactions in general and as an interesting case of strong solvent−solute coupling.[1−16] It has long been known that the solvent plays a decisive role in the reaction, both in providing a suitable environment and as a reactant, accepting the proton from the excited naphthol.

Modern cluster and laser-spectroscopy techniques have led to progress in understanding the 1-naphthol/water ESPT reaction. Recently, a detailed model of the intra- and intermolecular processes leading to the EPST reaction has been proposed for water as solvent.[16] The model was based on the discovery of vibrationally induced coupling of the first two electronically excited singlet states of free naphthol. This coupling provides a mechanism by which excitation to the S_1 state can, via electrostatic interaction with the surrounding water, result in inversion of the S_1/S_2 (L_a/L_b) electronic-state ordering, a dramatic increase in the (electronically excited) naphthol dipole moment, and finally excited-state proton transfer.

Although the model was supported by the available evidence, it was not possible to spectroscopically verify the importance of vibronic coupling in bulk liquid, since the single-vibrational-level resolution of a molecular-beam experiment is not available in solution.

The present work continues our effort to understand how complexation with water affects vibrational and vibrational−electronic coupling in this important prototype molecule. It is known that 1-NpOH·$(H_2O)_n$ clusters vary nonmonotonically in their properties up to $n = 7$, after which there is a smoother trend up to $n = 25$.[9] At this point the cluster is in some respects solution-like, as evidenced by the occurrence of the ESPT reaction.[9] The $n = 1$ complex is far from this limit, and not representative of bulk solution, but still illuminates the details of water interaction with this solute. In particular, the effect of a single water could be rather large, since it could lower the more polar S_2 state and increase the propensity for vibronic coupling. This effect has been observed for certain conformers of hydrogen-bonded indole complexes.[17] On the other hand, complexation could so modify the naphthol normal coordinates that vibronic coupling is reduced or eliminated.

Other related complexes have already received some attention, the most widely studied being phenol·H_2O.[18−32] These efforts have mostly focused on the fluorescence or multiphoton-ionization excitation spectra, particularly in the S_1 origin region. Several intermolecular modes are spectrally active, providing a test case for theoretical treatment of hydrogen-bonded complexes.[27,28] Pump−probe[22,23,30] and IR−UV double-resonance[32] methods have been used to study the kinetics of

* Corresponding author.
† ETH Zürich.
‡ Universität zur Köln.
§ Universität Bern.

S1089-5639(97)02069-0 CCC: $15.00
Published on Web 02/24/1998

S_1-T_1 intersystem crossing, but otherwise, little is known about the dynamics in the excited state. In addition to dispersed fluorescence studies,[24,28] the ground state has been probed by ion-dip spectroscopy (IDS), which revealed intramolecular vibrational relaxation at 813 cm^{-1} in the S_0 and strong coupling of intermolecular modes in the S_1.[24−26,29]

Yet more closely related is the 2-naphthol·H_2O complex, which has been the object of a recent theoretical and experimental study.[33] In this complex the intermolecular vibrations are readily observed in both absorption and emission and are different in the cis and trans isomers, making a detailed analysis possible. The study was, however, not extended to higher vibrational levels in the excited state nor were any dynamics observed.

Excited-state intramolecular vibrational redistribution (IVR) has been observed via quantum beats in free 1-naphthol at excess energies of 1100 cm^{-1} or greater.[34] Although there have been numerous studies of excited-state proton-transfer dynamics in naphthol and phenol clusters with polar solvent molecules,[12,13,35−39] little is known about the dynamics of higher single vibrational levels in naphthol·H_2O or other classical hydrogen-bonded (aromatic—X—H···X—, X = O,N) complexes. Changes in decay rates and L_a/L_b coupling versus level-specific vibrational excitation in ammonia clusters of 3-methyl indole is one of the few such examples.[40]

Intramolecular vibrational redistribution has been a major topic in molecular physics for many years. Much effort has gone into characterization of covalently bound molecules and their excited states, since these are the most accessible. The density of states has emerged as the dominant factor leading to IVR in most cases. This has led to experiments such as modifying the number of "bath" states coupled to a chromophore by changing the length of the aliphatic "tail" attached to a benzene ring and observing the effect on the IVR threshold.[41−43] The results were interpreted in terms of separated manifolds of ring and tail (bath) vibrational modes, a crucial distinction for both qualitative understanding and theoretical modeling. Recently, this assumption of separated manifolds has been cast into serious doubt by more detailed studies of these molecules.[44] More recent studies of smaller nonaromatic molecules have shown less dependence on the density of states, though this may have to do with the initial-state preparation method.[45] Clusters offer potentially more separated manifolds, and complexes of aromatics with rare-gas atoms and small molecules have received significant attention.[46−61] Particular progress has been made on s-tetrazine[47,52−54] and p-difluorobenzene[55−57] complexes, for which a sequential IVR/predissociation model has proved particularly successful.[49,50,58] However, the rare-gas atoms sit on the π-electron system and are therefore not so well isolated from the electronic transition as could be desired. Hydrogen-bonded systems such as the present 1-naphthol·H_2O could be yet better, despite a higher binding energy, since the water is coupled to the π system only through the −OH group.

Ground-state IVR has been widely studied because of its relevance to schemes for mode-selective chemistry via infrared excitation.[62,63] The extent to which ground- and excited-state IVR of the same molecule are similar has, however, received much less attention. In the ring-and-tail systems it was concluded that ground-state IVR is broadly the same as in the S_1 and dominated by a density-of-states effect.[64] As noted above, the phenol·H_2O complex has been shown to undergo IVR in the ground state,[24,26,29] but the corresponding excited-state behavior is not known and is complicated substantially by rapid intersystem crossing. This complication is not an issue for small naphthol·$(H_2O)_n$ clusters, which all have long singlet lifetimes.[9] In tetrazine·Ar much faster IVR was found in the S_1 than the S_0,[52,53] which was attributed to a difference in the modulation of the intermolecular potential by ground- and excited-state vibrations. Other workers have pointed out the importance of rotational levels and mixing of van der Waals modes in modulating IVR in this complex.[47]

Experimental and Computational Methods

Experiment. The experimental method was very similar to that reported in earlier studies on this molecule.[9,12,13,15,16] We present only a very brief summary. 1-Naphthol (1-NpOH) was entrained in a stream of neon/helium carrier gas at a partial pressure of <3 mbar, and the total stagnation pressure was 1−1.5 bar. This mixture was passed through a pulsed valve into a vacuum. The expansion-cooled molecules were then interrogated with nanosecond pulses from a frequency-doubled pulsed dye laser (Lambda Physik FL-2002 or 3002) using DCM dye. The water complexes were generated by adding 1−20 mbar of water vapor to the gas stream.

The one-color resonant two-photon ionization (R2PI) spectra were obtained by crossing the skimmed molecular beam with the unfocused doubled dye-laser pulses inside the acceleration region of a 1-m linear time-of-flight mass spectrometer. The acceleration voltage used was 5 kV, and the ions were detected with a microsphere plate (El-Mul Technologies, Israel). The laser was scanned while the relevant mass peak was observed with a transient digitizer.

Two-color ion-dip spectroscopy[65] was performed by crossing the beams from two doubled dye lasers in the acceleration region of the mass spectrometer. The pump beam was fixed on an absorption of the complex and attenuated until the one-color R2PI signal virtually vanished. The dump beam was scanned to lower energy and focused with a 50-cm lens to achieve the maximum depletion possible. Despite the focusing, no one-color signal from this laser was observable. The relatively low ionization potential and slowly varying photoionization efficiency[11] of the 1-naphthol·H_2O complex enable efficient ion-dip spectroscopy over a wide energy range.

The fluorescence was dispersed with SPEX 0.5- or 1.0-m grating monochromator (3600 or 2400 lines/mm gratings, respectively) and detected with a photomultiplier (Hamamatsu R106 or R928). The spectral band-pass was varied from 10 to 20 cm^{-1} as necessitated by signal levels.

Computations. Full geometry optimizations were performed at the Hartree−Fock SCF level with the 6-31G(d,p) basis set using the Gaussian-92 program package.[66] The most stringent optimization criteria were used (very tight option of $<10^{-6}$ au for the norm of the gradient). Analytical second derivatives were calculated at the SCF equilibrium structure, and a normal-coordinate analysis was performed, yielding harmonic frequencies and normal-mode eigenvectors for both 1-naphthol·H_2O and 1-naphthol-OD·D_2O.

Results and Discussion

Calculated Geometry and Vibrational Analysis. *A. Complex Geometry*. Some important intermolecular structural parameters of the complexes are given in Table 1. Comparing intermolecular bond lengths and angles for 1-naphthol·H_2O with those of phenol·H_2O,[28] *trans*-2-naphthol·H_2O,[33] and the water dimer,[33] one notices the following: the hydrogen bond length R(O···O) contracts considerably by 0.08 Å on going from $(H_2O)_2$ to phenol·H_2O and is almost the same in phenol and *trans*-2-naphthol complex but is yet shorter in 1-naphthol·H_2O.

TABLE 1: Structural Parameters of the 1-Naphthol·H_2O Complex As Calculated at the 6-31G (d,p) Level[a]

	1-NpOH·H_2O	*trans*-2-NpOH·H_2O	Ph·H_2O	$(H_2O)_2$
O···O bond length	2.894	2.904	2.906	2.980
angle of water plane vs O···O axis	132.8	135.2	135.79	117.6
hydroxyl C−O−H angle (or HOH)	111.5	111.8	111.6	105.9
angular deviation of donor OH bond from O···O axis	3.2	3.4	3.3	5.3

[a] Comparable parameters calculated at the same level are shown for phenol·H_2O,[28] *trans*-2-naphthol·H_2O,[33] and $(H_2O)_2$.[33] The distances are in angstrom and angles are in degrees.

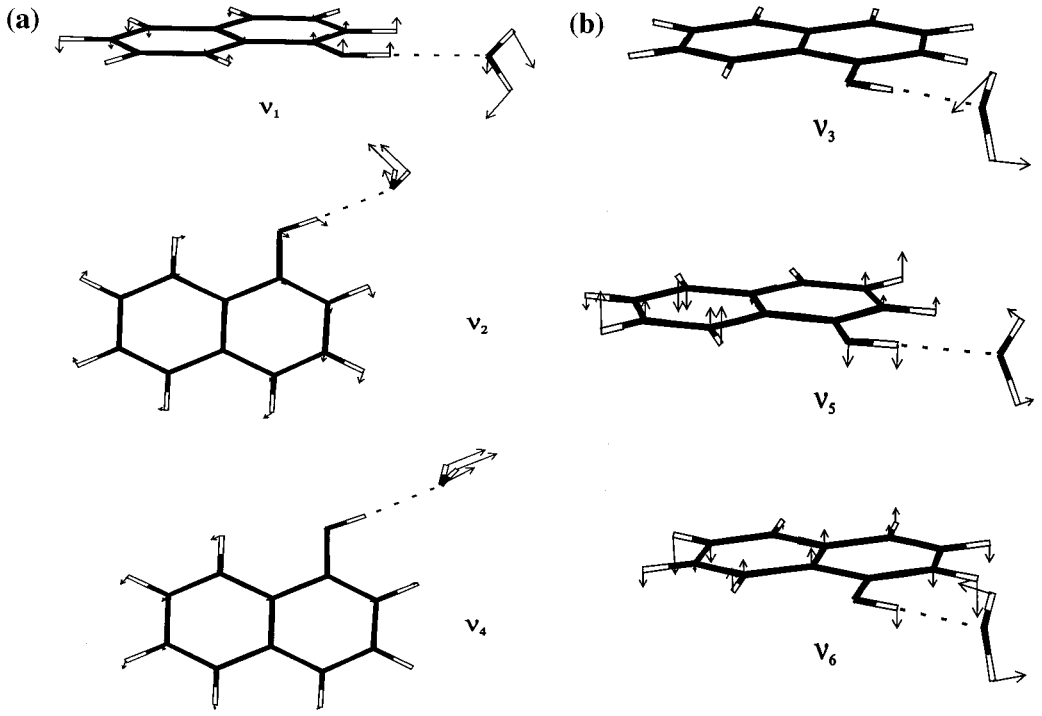

Figure 1. Intermolecular vibrations of the 1-naphthol·H_2O complex as calculated at the 6-31G(d,p) level. See Tables 1 and 2 for the corresponding geometrical parameters and frequencies.

The angle between the bisector of the H_2O molecular plane and the O···O axis decreases very slightly in this sequence of hydroxy aromatics. The angle between the donor O−H bond and the O···O axis remains essentially constant. The intramolecular geometry parameters (aromatic molecule O−H bond lengths and bond angles) change even less and are similar to those of phenol[28] and *cis*- and *trans*-2-naphthols.[33]

B. Intermolecular Vibrations. Six intermolecular normal modes arise from complexation of 1-naphthol with an H_2O or D_2O molecule. Figure 1 displays the calculated intermolecular normal modes of 1-naphthol·H_2O. As for phenol·H_2O and 2-naphthol·H_2O, the calculated modes can be divided into two classes. (i) One class is translational-type modes characterized by large reduced masses and small deuteration shifts. These are the low-frequency rock, ρ_1, the low-frequency bend, β_1, and the hydrogen-bond stretch, σ. (ii) The other class is rotational-type modes characterized by small reduced masses and large deuteration shifts, which are the high-frequency rock, ρ_2, the high-frequency bend, β_2, and the torsion, τ. The calculated intermolecular harmonic vibrational frequencies range from 25 to 172 cm^{-1} for 1-naphthol·H_2O and from 23 to 152 cm^{-1} for naphthol-OD·D_2O. For the latter, the lowest intramolecular mode appears at 152 cm^{-1} and overlaps with the intermolecular modes. Table 2 compiles the intermolecular frequencies for 1-naphthol·H_2O and naphthol-OD·D_2O and compares them to the frequencies calculated for *trans*-2-naphthol·H_2O[33] and phenol·H_2O.[27,28] Apart from the lowest-frequency rocking mode, ρ_1, all intermolecular frequencies of 1-naphthol·H_2O are

TABLE 2: Intermolecular S_0 Vibrational Frequencies Calculated at the 6-31G (d,p) Level for 1-Naphthol·H_2O, 1-Naphthol-OD·D_2O, *trans*-2-Naphthol·H_2O,[33] and Phenol·H_2O[28] [a]

	1-NpOH·H_2O	1-NpOD·D_2O	2-NpOH·H_2O	Ph·H_2O
ν_1 a″ ρ_1 rock	25.2	23.4	24.8	30.3
ν_2 a′ β_1 bend	49.6	46.0	54.4	53.1
ν_3 a″ τ torsion	90.9	64.5	108.6	93.3
ν_4 a′ σ stretch	127.0	118.7	146.5	139.7
ν_5 a″ ρ_2 rock	139.7	135.2	228.5	193.9
ν_6 a′ β_2 bend	172.2	151.0	211.0	202.1

[a] The units are wavenumbers.

significantly lower than those of 2-naphthol·H_2O, namely, by 9% for the bend β_1, by 16% for the torsion, by 13% for the intermolecular stretch, by 39% for the high-frequency rock ρ_2, and by 18% for the high-frequency bend β_2. These very significant changes reflect both geometric and mass factors, that is, larger reduced masses for the intermolecular vibrations, and do *not* imply that the intermolecular force constants are significantly different between these two naphthol isomers. However, the mass/geometry (**G** matrix) changes do imply larger coupling of intra- and intermolecular modes in this system compared to 2-naphthol.

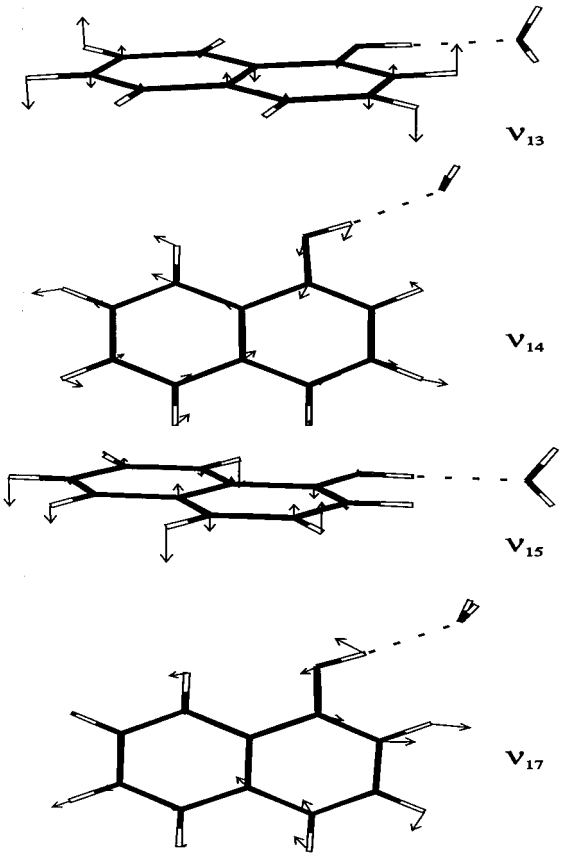

Figure 2. Some intra-naphthol vibrations of the 1-naphthol·H_2O complex as calculated at the 6-31G(d,p) level. The ν_{13} vibration is spectrally active even though it is a″ symmetry, i.e., out-of-plane. The ν_{14} vibration most closely resembles the vibronically active mode in free 1-naphthol[16] and becomes mixed with ν_{15} as a result. The ν_{17} vibration undergoes relatively weak IVR in the S_1 state. The calculated frequencies are $\nu_{13} = 468$, $\nu_{14} = 472$, $\nu_{15} = 521$, and $\nu_{17} = 577$ cm^{-1}. The observed frequencies in the ground state are $\nu_{13} = 467$, $\nu_{14} = 477$, $\nu_{15} = 510$, and $\nu_{17} = 570$ cm^{-1}.

Figure 2 shows some calculated intra-naphthol vibrations of the 1-naphthol·H_2O complex. These were selected for their relevance to aspects of the spectroscopy as discussed below. As is apparent from the figure, in the important energy range there is essentially no coupling of the naphthol motions to the water. This separation of harmonic coordinates appears to be qualitatively better than in the classic ring-and-tail systems previously studied.[41−45]

Absorption Spectra. The two-photon ionization spectrum of 1-NpOH·H_2O is quite similar to that of free 1-NpOH, as is seen in Table 3. There are remarkably few additional bands due to intermolecular vibrations, notably at 57 cm^{-1} (54 cm^{-1} for the deuterated complex) above the S_1 origin. This is assigned as the β_1 a′ hydrogen-bond bend, with a (S_0) calculated frequency of 49.6 (46.0) cm^{-1}. The β_1 bend is observed in spectra of several hydroxyaromatic·water complexes.[19,20] Another assignment, although less likely, is as two quanta of the ρ_1 a″ rock at 2×25.2 cm^{-1}. This might be the weak shoulder observed 2.5 cm^{-1} to lower energy. Either of these would have the requisite symmetry to be active, as well as a small isotope shift consistent with the calculated motions. Since the lowest two vibrations involve the whole water molecule, a shift due to the mass difference of $(20/18)^{1/2} = 1.054$ is expected very near the observed $\nu_a/\nu_b = 57$ cm^{-1}/54 cm^{-1} = 1.055. This intermolecular mode is also apparent in a combinations with intra-naphthol modes at 402 and 495 cm^{-1}.

TABLE 3: Some Vibrations Observed in Resonant Two-Photon Ionization of 1-Naphthol·H_2O/D_2O, in Wavenumbers, above the $S_1 \leftarrow S_0$ Electronic Origin[a]

1-naphthol	1-naphthol·H_2O	1-naphthol-OD·D_2O
	57	54
207	209	205
276	292	291
		393
410*	400/403	399
		418
414*		
454	454	447
		450
		469
	459 (402 + 57)	
493	495	493
	501 (292 + 209)	
		514
	517 (402 + 2(57))	
547	547	539
	553 (495 + 57)	
		558
665	669	665
		682
684	694	692
		699
717	717	715
728	728	734
	755	763
761	771	
835	834	833
842		
864	854	852
		857
879	879	881
907	893	
951	949	966
1012	1012	1024

[a] The reference data for free 1-naphthol are taken mostly from ref 34. The 1-naphthol vibrations marked with an asterisk were found in ref 16 to be mixed by vibronic coupling. Some possible assignments as combinations including intermolecular vibrations are indicated in parentheses for 1-naphthol·H_2O.

The two-photon ionization spectrum of 1-NpOD·D_2O is somewhat more structured than that of its protonated counterpart, as can be seen from Table 3. This is also the case for uncomplexed NpOD versus NpOH. Much of this effect is believed to arise simply from changes in the reduced mass of the normal coordinates. The possible contribution of vibronic-intensity borrowing is currently under study. Combinations of intra-naphthol and intermolecular modes are not clearly identifiable in the 1-NpOD·D_2O spectrum.

Fluorescence Spectra. In contrast to the absorption spectra, the fluorescence spectra of the NpOH·H_2O complex after excitation to individual vibrational levels in the S_1 differ considerably from the corresponding NpOH spectra.[16,34] Only excitation of the lowest-lying (209 and 292 cm^{-1}) vibrational levels results in fluorescence spectra similar to those observed in free NpOH (see Table 4 and compare with Figure 1 of ref 16 and Figure 5 of ref 34). The spectra are dominated by the 1−1 ($\Delta v = 0$) transition in the excited mode. Scanning further to the red, one finds that the fluorescence spectra are also very similar to that of free NpOH.

This straightforward pattern is broken at an excitation energy of 402 cm^{-1} above the origin (such excitations will hereafter be denoted as $+nnn$ cm^{-1}). Here, there appears suddenly a broad group of partly overlapped bands in the region where a single strong $\Delta v = 0$ transition is expected. This is also the case at higher excitation energies, although the structure within

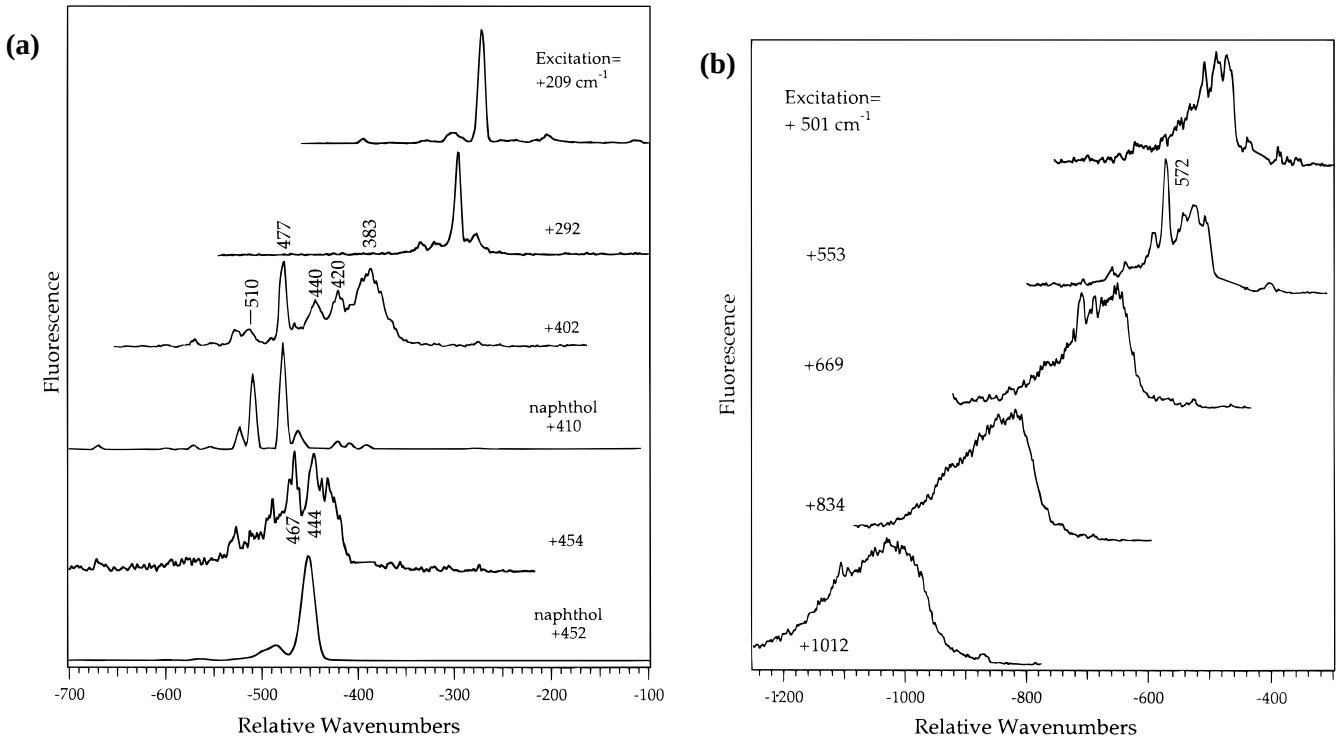

Figure 3. Fluorescence spectra of 1-naphthol·H_2O complexes excited at various energies above the S_1 origin. The data are plotted relative to the excitation energy to show the ground-state vibrational energies of the final states. See Table 4 for a list of the emission bands. Below 400 cm^{-1} excess energy, the spectra resemble those of the free naphthol molecule. Above 400 cm^{-1} excess energy, restricted IVR leads to a mixture of relaxed and unrelaxed emission. In some spectra bands due to free 1-naphthol have been deleted. Two 1-naphthol spectra are included for comparison.

the asymmetric band profile slowly becomes washed out by a general broadening. Even excitation at +501 cm^{-1} follows this pattern, although this excitation is a combination of the 209 and 292 cm^{-1} vibrations.

The structure observed in each case is not similar, as would be expected if it were due to progressions in low-energy intermolecular modes. Some bands can be assigned to known ground-state vibrations; the dominant emission band is usually that expected from the free naphthol spectrum, where only the 1−1 transition from the excited level is observed. The ground-state complex vibrational energies and the corresponding naphthol values are compiled in Table 4. Some of the calculated ground-state normal modes in this frequency range are shown in Figure 2.

The +402 cm^{-1} absorption band is found to be somewhat special in that it is composed of two nearly degenerate levels. As shown by fluorescence excitation spectroscopy in Figure 4, the unresolved +402 cm^{-1} absorption seen in R2PI is in fact a superposition of two absorption bands, separated by about two wavenumbers, and strongly overlapped. The level at +403 cm^{-1} contributes strongly to the emission to the ground-state levels at 420, 440, 477, and 510 cm^{-1} shifts, while the level at +400 cm^{-1} contributes more the broad fluorescence peaked at 383 cm^{-1} shift in Figure 3.

Intracomplex S_1 Vibrational-Energy Redistribution (IVR). The pattern of assignable and unexpected bands found in the fluorescence spectra above 400 cm^{-1} excess energy is typical for "restricted" intramolecular vibrational redistribution as observed in rigid molecules.[48,67] The low-energy intermolecular modes combined with the intra-naphthol vibrations lead to a vibrational density of states (DOS) that rises very rapidly in the complex as a function of excess energy. In free naphthol the first signs of IVR, in the form of spectral broadening or quantum beats, were observed at about 1100 cm^{-1} above the origin,[34] where the vibrational DOS is about 2 per wavenumber, as calculated by a direct-count algorithm[68] and assuming harmonic vibrations. By use of the calculated ab initio frequencies and the direct-count method, the same DOS is found in the water complex at about 400 cm^{-1}, making the observed spectra very understandable at first glance. We return to this topic below in the context of ground-state IVR. At the upper end of the excess energy range shown in Figure 3, the DOS is about 10 per wavenumber and the transition to "dissipative" IVR is clearly in progress, as seen from the substantial broadening in the fluorescence spectra.

IVR is typically a general phenomenon at all excitation energies above its first appearance.[69] However, the two levels +400 and +403 cm^{-1} show differing IVR behavior even though they are nearly degenerate. These two vibrations are the closest in energy to the vibronically active, Duschinsky rotated +410 and +414 cm^{-1} modes of free 1-naphthol.[16,34,70] The unrelaxed emission would be dominated by the pair of bands at 477 and 510 cm^{-1} (compare the 1-naphthol +410 cm^{-1} fluorescence spectrum in Figure 3a). The unrelaxed emission is indeed relatively strong when exciting at +403 cm^{-1} but becomes much weaker when exciting more of the +400 cm^{-1} level, as seen in Figure 5 for excitation at +401 cm^{-1} (Figure 5b) or at +398 cm^{-1} (Figure 5c). Also in contrast with the +400 cm^{-1} level, the +403 cm^{-1} level shows discrete emission bands to ground-state levels at 420 and 440 cm^{-1}. This is limited IVR rather than a further Duschinsky rotation involving levels other than that at +400 cm^{-1}. Such a Duschinsky rotation would imply corresponding bands in absorption, which are not found. From the lack of structure in spectrum c of Figure 5, the +400 cm^{-1} level would seem to undergo remarkably strong, nearly dissipative IVR.

In addition to its ubiquity above threshold, the extent of IVR also typically increases monotonically with excitation energy as the underlying vibrational DOS rapidly increases.[69] The fluorescence spectrum after excitation at +553 cm^{-1} is therefore

TABLE 4: Ground-State Vibrations Observed in the Origin-Region Fluorescence after Excitation to the Indicated S_1 Vibronic Levels of 1-Naphthol·H_2O[a]

excitation above 0−0 in H_2O complex	1-NpOH·H_2O fluorescence	1-NpOH·H_2O calculated	1-NpOH fluorescence
		189	
		204	
209	274	267	274
292	295	298	281
		424	
		458	
400	383/420/477/510/523	472	478/510
454	444/467/488/528	467	465
493	467/528	521	524
		563	
501	467/488/509		not observed
553	509/524/572/590/638/670	577	573
		641	
		659	
669	602/688/714	701	715
		743	
		770	
		782	
		804	
834	812/845	856	
875			874/955/983
		893	
		977	
		985	
		993	
		1012	
1012	1030/1106	1026	1040

[a] The calculated values for the water complex and the measured free naphthol ground-state vibrational frequencies are presented for comparison. See Table 3 for the naphthol excitation energies. Complex vibrations that are also observed in fluorescence from the S_1 origin are underlined. The units are wavenumbers.

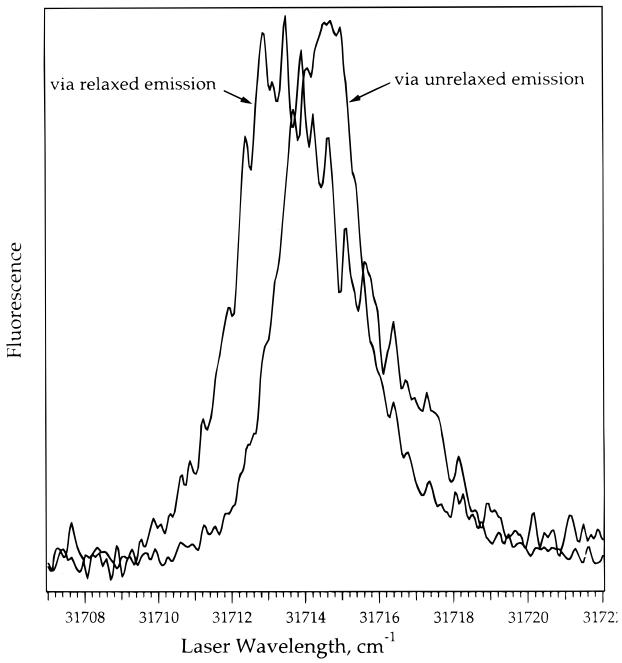

Figure 4. Fluorescence excitation spectra of the absorption bands near 400 cm^{-1} excess energy. The 31 715 cm^{-1} (403 cm^{-1} above the origin) absorption was observed via the narrow unrelaxed fluorescence at 477 cm^{-1} shift (see Figure 3). The 31 713 cm^{-1} excitation (400 cm^{-1} above the origin) could be observed via shorter emission wavelengths (shifts of 400−450 cm^{-1} in Figure 3). In addition, both of these absorptions contribute to the peak of the relaxed IVR emission at 383 cm^{-1} shift.

unusual, since it is more structured than the spectra following excitation at both higher and lower excess energies. As seen in Figure 3b, the fluorescence is dominated by the 572 cm^{-1} band, which is the $\Delta v = 0$ transition from the nominally prepared vibration. It thus represents a partially "frozen" mode, 150 cm^{-1} above the IVR threshold. The calculated atomic displacements in this normal mode (ν_{17}) are shown in Figure 2. This is quite rare; analogous examples of limited mode specificity in IVR are combinations with the ν_{30} vibration of *p*-difluorobenzene[69] and the 867 cm^{-1} mode of 2,5-diphenylfuran.[46] In the first case, the ν_{30} vibration *enhances* IVR. In diphenylfuran the 867 cm^{-1} vibration remains less affected by IVR than lower energy levels, even when the DOS is increased by complexation with argon. However, in the argon complex it does couple to the bath on a time scale of 250 ps. In the present case, the initially prepared state is much more durable; it must persist over many nanoseconds to be observed so strongly in our experiment.

Our observation of restricted IVR in the NpOH·H_2O hydrogen-bonded complex at the same DOS where such effects are observed in rigid molecules such as anthracene[67] is significant. Although IVR induced by very low frequency modes in molecules has been systematically studied,[41−45] van der Waals and hydrogen-bonded complexes are rather different in that these modes are present in a part of the complex that is not covalently bound to the chromophore. NpOH·H_2O is also different from van der Waals complexes[46−61] in that the water is not adjacent to the π-electron system. This type of IVR may be considered as a step toward direct observation of intermolecular vibrational relaxation in polar bulk solution if we regard the water as solvent and the naphthol as solute. Although hydrogen-bonded clusters and complexes have been widely studied, little is known about their IVR thresholds. As noted in the Introduction, the phenol·H_2O complex has a threshold in the ground state between 527 and 825 cm^{-1}, where the DOS is substantially higher than here, between 7 and 44 /cm^{-1}.[24] How this differs from the free phenol is not known. Isoquinoline complexes with water and

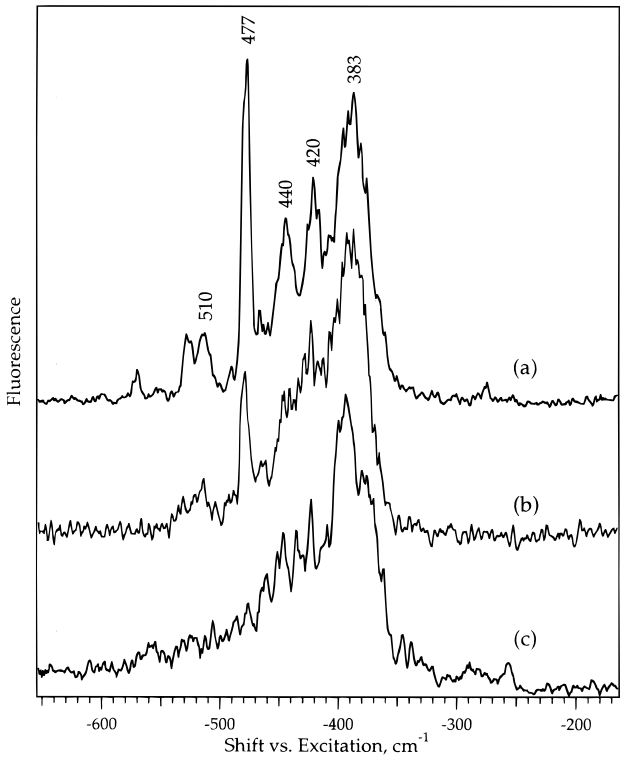

Figure 5. Fluorescence spectra after excitation near 400 cm^{-1} excess energy. Trace a results from excitation at 403 cm^{-1} excess energy. The unrelaxed emission to the 477 and 510 cm^{-1} ground-state levels is strong. Trace b results from excitation at 401 cm^{-1} excess energy. Although unrelaxed emission is weaker, the 477 cm^{-1}/510 cm^{-1} intensity ratio decreases as expected. Exciting on the absorption edge at 398 cm^{-1} excess energy leads to trace c, with no unrelaxed emission remaining.

methanol show a sudden drop in fluorescence lifetime for vibrational levels higher than about 1000 cm^{-1} in the S_1,[71] but this is may or may not be directly correlated with IVR. Decay-rate dependence on vibrational excitation in ammonia clusters of 3-methylindole is probably related to IVR but is complicated by L_a/L_b electronic-state coupling.[40]

Assignment of IVR "Bath" Modes. In some previous studies of chromophore-bath energy IVR studies it was not possible to say much about the mechanism of IVR because of the lack of information about these "bath" modes. Such information is available for van der Waals complexes with monatomic gases but has seldom been fully utilized. For example, sequential IVR−vibrational predissociation in several van der Waals clusters has been successfully treated by a model that takes into account individual chromophore vibrations and includes the intermolecular vibrations primarily via the DOS they generate.[49,50] In another case, a perturbation-theory analysis of IVR in tetrazine·argon focused on the changes in chromophore vibrational occupation numbers, after excitation at high excess energies.[52] The naphthol·water case is unusual in that a small set of reasonably well-characterized modes (the intermolecular vibrations) are responsible for a low IVR threshold. Within a first-order anharmonic model for IVR, this allows us to narrow the range of possible IVR bath states far more than is generally possible.

The structure in IVR spectra can generally be assigned to any level having the proper energy. This could be a sum of many low-energy intermolecular "bath" excitations or one quantum of an intra-naphthol mode with a few quanta of intermolecular modes. Only the latter is consistent with lowest-order anharmonic coupling, as discussed by Gruner, Nguyen, and Brumer[72] for the case of anthracene. We next apply this model to the first IVR-active levels of excited naphthol·H_2O, where the DOS is still relatively low, where only a few levels are coupled and where lowest-order descriptions should be the most valid.

Let us denote the occupation numbers of the unmixed vibrations as $|jkl...mn\rangle$. The lowest modes *j, k, l* represent the intermolecular vibrations, while the higher ones *n* and *m* are representative of the intra-naphthol modes. As shown in ref 72, anharmonicity mixes the S_1 vibrational level $|000...01\rangle$ with others differing by one or three quanta and that are nearby in energy. No states involving changes in quantum number of 1 are energetically relevant here; the possible levels differing in quantum numbers by 3 are $|020...00\rangle$, $|101...00\rangle$, or $|001...10\rangle$. These lead to "new" structure in the fluorescence spectra. Furthermore, $|000...01\rangle$ excitations in the intermediate IVR range should mix only with states such as $|010...10\rangle$ rather than pure "bath" states $|002...00\rangle$ or $|101...00\rangle$, since the highest such two-quantum intermolecular bath state is calculated to be at $2 \times 172.2 = 344.4$ cm^{-1}, well below the onset of IVR.

Consider now the excitations $|000...01\rangle$ at +400 and +403 cm^{-1}. As noted above, the +403 cm^{-1} level is much more IVR-active. Let it be coupled by anharmonicity to a combination state $|010...10\rangle$ in the S_1 electronic state, which then fluoresces to the S_0. In Figure 3 we observe the $\Delta v = 0$ region of the fluorescence spectra, so the S_0 vibrational occupation numbers are also $|010...10\rangle$. We observe the major peak in the fluorescence corresponding to an S_0 vibrational state at 383 cm^{-1}. A candidate intra-/intermolecular combination would be one quantum of the 295 cm^{-1} intra-naphthol mode combined with an intermolecular mode at 88 cm^{-1}. The latter is near the calculated value for the torsion motion. The only other possible assignment is 211 + 172 (a′ β_2 bend). This intra-naphthol vibration is not far from a calculated mode at 204 cm^{-1}. The combination with the torsion mode is possibly more likely, by analogy to the rather general promotion of IVR by methyl rotors.[58,63] To be nearly degenerate with the pumped S_1 level, increases in the intermolecular mode frequencies in the S_1 state are required. Such increases were observed in the closely related 2-naphthol·water,[33] by about 10 cm^{-1}. Somewhat larger but reasonable increases would achieve near-degeneracy here.

Other emission bands resulting from restricted IVR appear at 420 and 440 cm^{-1} shifts when the +400 cm^{-1} (but not +403 cm^{-1}) S_1 level is excited. For the 440 cm^{-1} ground-state level, the likely combination is the 274 cm^{-1} intra-naphthol vibration with the 172 cm^{-1} a′ β_2 intermolecular bend. With the decrease in the intra-naphthol mode energy to 209 cm^{-1} and a ∼10% increase in the intermolecular frequency, this combination is at 398 cm^{-1} in the S_1, quite near the pumped level.

For the 420 cm^{-1} band the possible anharmonically coupled S_0 combination states are the 274 cm^{-1} intra-naphthol vibration with the a″ ρ_2 intermolecular rock at 145 cm^{-1} (calculated to be at 140 cm^{-1}) or 295 + 127 (a′ intermolecular stretch). In the former combination, although the 274 cm^{-1} S_0 mode drops to 209 cm^{-1} in the S_1, the ρ_2 intermolecular rock may increase from from 145 to 191 cm^{-1} in the S_1. We rule out the latter combination because the 295 cm^{-1} vibration is nearly isoenergetic in the S_0 and S_1 states, so the corresponding S_1 combination will lie 20 cm^{-1} above the pumped +400 cm^{-1} level. This obviously cannot be compensated by the expected increase in intermolecular frequency.

For +454 cm^{-1} excitation, the strong 444 cm^{-1} emission band may be assigned as 274 + 172 cm^{-1} (β_2 bend), 295 + 145 cm^{-1} (a″ ρ_2 rock), or 424 + 25 cm^{-1} (a″ ρ_1 rock). Of these

the 295 + 145 cm^{-1} combination is clearly the most acceptable, since the S_1 frequency should be near 452 cm^{-1}.

In summary, of the four strong, discrete bands resulting from IVR in the spectra of the two lowest IVR-active S_1 levels, three can be assigned or strongly constrained using energy considerations in the S_0 and S_1 states in combination with the anharmonic selection rules of Gruner, Nguyen, and Brumer.

Vibronic Coupling: Quenching and Enhancement versus Free 1-Naphthol. The 400 and 403 cm^{-1} excited-state vibrations are of particular interest, since they are the closest in energy to the vibronically active +410 and +414 cm^{-1} modes of free 1-naphthol.[16,34,70] In free 1-naphthol, excitation of either one of these levels resulted in strong crossed-sequence emission bands, of which the strongest terminated at 477 and 510 cm^{-1} levels in the ground state (see Figure 3). This was in turn found to be indicative of vibrational mixing of S_2 character into the S_1 electronic state. In the water complex, excitation at +403 cm^{-1} also results in fluorescence to the two expected ground-state levels at 477 and 510 cm^{-1} but not with the expected nearly equal intensity ratios. We conclude that the coupling has been reduced by complexation with a single water molecule. This is interesting, since the presence of the water molecule might be expected to lower the more polar S_2 state relative to the S_1. In a perturbative view this would enhance vibronic coupling, all other factors being equal. As will be discussed below, harmonic-mode mixing probably is a factor, so this argument is too simple. However, it cannot even be assumed that the water will decrease the S_2-S_1 splitting. In polar complexes with indole, it was found that if the solvent molecule is the proton *acceptor* in a hydrogen bond, the S_2 is not affected by complexation.[17] The S_2-S_1 splitting is, however, dramatically reduced if the solvent is a proton *donor*. The 1-naphthol·H_2O complex seems to fit this picture: the water is a proton acceptor and there is no evidence for a low S_2.

That the two S_1 vibrations in the complex are at essentially the same energy, yet are less strongly coupled than when 4 cm^{-1} apart in the free naphthol, is another confirmation of the earlier conclusion[16] that the coupling is not a Fermi-type perturbation but rather a vibronically induced Duschinsky rotation[74] of the normal modes. The 477/510 ratio appears to decrease when moving from +403 cm^{-1} toward +400 cm^{-1}, as seen in Figure 5. By analogy to free naphthol, strong 510 cm^{-1} emission would eventually be expected but is never observed because of the dominance of IVR for +400 cm^{-1} excitation.

The weak S_1/S_2 coupling in the complex is a consequence of changes in the naphthol ring motions, either due to the increased mass attached to the 1-position or due to changes in the intra-naphthol potentials resulting from the hydrogen bond. As seen in the fluorescence spectra of the NpOD·D_2O complex in Figure 6, isotopic substitution to increase the pendant mass seems to *increase*, rather than decrease, the vibronic coupling. The 510 cm^{-1} band appears with as much as half the intensity of the 477 cm^{-1} band, or roughly twice as strongly as in the protonated complex, though still not so strongly as in the free molecule. This suggests that the water affects the vibration inducing the coupling primarily via its mass (harmonic-mode mixing[75]) rather than by modifying force constants through hydrogen bonding. Similarly, vibronic coupling in free 1-NpOD is as strong or somewhat stronger as in 1-NpOH.

In contrast to the quenched vibronic coupling of the +400/+403 cm^{-1} pair, there are indications of increased vibronic coupling in the S_1 292 cm^{-1} vibration versus free naphthol. As seen in Figure 3, surrounding the main emission are a number of smaller bands, covering a substantial energy range from 11 cm^{-1} below to 26 cm^{-1} above the main peak. These are all coupled together in the S_1, as is apparent from the fluorescence excitation spectrum of Figure 7, observed at the main fluorescence peak. When observing at a secondary emission peak, as seen in the lower spectrum, the smaller absorptions are relatively

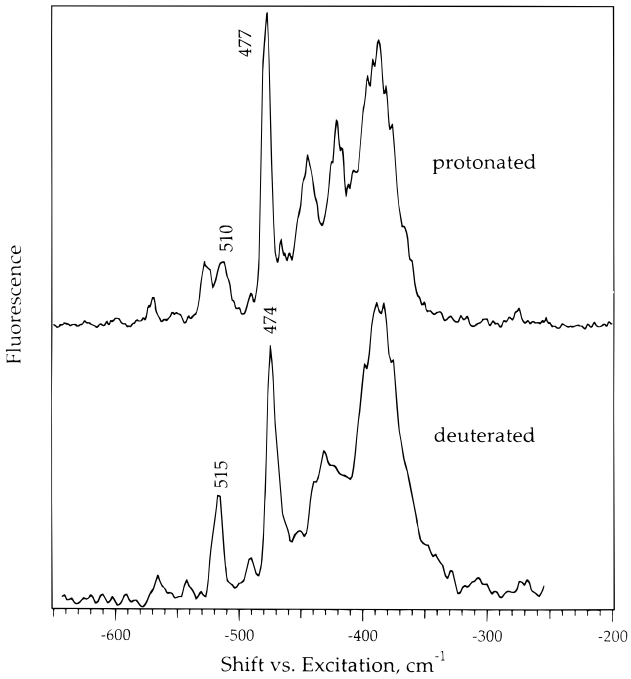

Figure 6. Fluorescence spectra of 1-naphthol·H_2O (upper) and 1-naphthol-OD·D_2O (lower) clusters after excitation of the origin +402 or +398 cm^{-1} bands, respectively. In the protonated complex there is little evidence for vibrationally induced coupling of the S_1 and S_2 states, as was observed in free naphthol,[16] as indicated by the lack of strong crossed-sequence emission at 510 cm^{-1} shift. Stronger coupling is observed in the deuterated complex (see text for discussion).

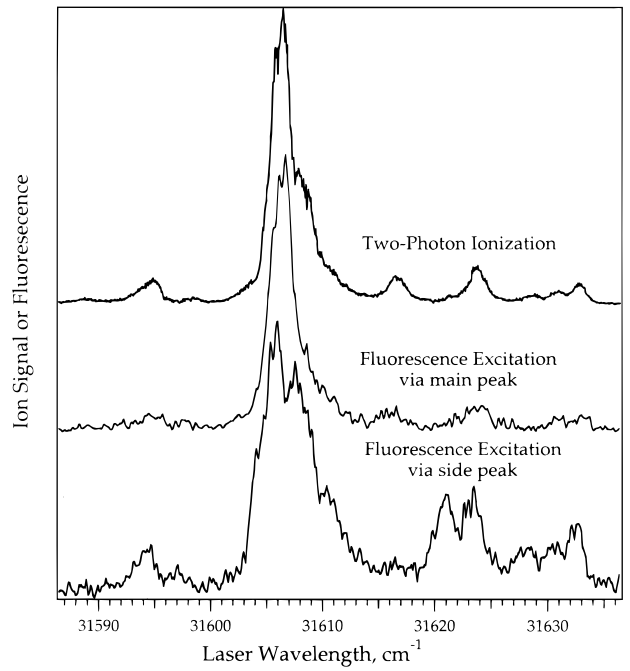

Figure 7. Resonant two-photon ionization and fluorescence excitation spectra of the origin +292 cm^{-1} band of the 1-naphthol·H_2O complex. The excitation spectrum was taken while observing the peak of the emission, at 295 cm^{-1} in Figure 3. The similarity of the structure indicates that the numerous absorptions represent a coupled set of vibrational states.

enhanced, as expected for a coupled group. The energy range spanned in absorption is quite large for simple Fermi coupling, though this may play a role in the appearance of the shoulder on the main absorption peak. The remaining structure seems more likely to be the result of a different perturbation of longer range. Vibronic coupling is a strong candidate, since it can give intensity to otherwise dark bands throughout the spectrum,[76] yet there is a also a nearness propensity.[74]

Ion-Dip Spectroscopy: Vibrational-Energy Redistribution in the Ground State. As seen above, S_1 IVR in NpOH·H_2O begins at an excess energy where the DOS reaches about 2 per wavenumber. Although the +400 and +553 cm^{-1} modes are interesting special cases, the DOS initially appears to be the dominant factor determining the strength of IVR, as in rigid molecules. A corollary of this is that IVR should be very similar in the ground state, as was found for the ring-and-tail systems.[64] On the other hand, electronic (excited state) structure dependence of IVR has been found in a series of *p*-alkoxyaniline molecules,[77] so it cannot be taken for granted that this will be so. Very large S_1 versus S_0 differences in IVR rates were also found for tetrazine·Ar due to modulation of the intermolecular potential by ring vibrations.[52,53]

Ion-dip spectroscopy can address this question to a limited extent. For fluorescence bands of sufficient oscillator strength, a strong dump laser can saturate the transition, leading to a maximum dip in the absence of IVR of 50%. If the lower state is depleted by relaxation into other states by IVR, then a deeper dip can be observed. (Note that dissociation of the complex can be ruled out, since the ground-state binding energy has been measured to be 2035 ± 69 cm^{-1},[78] far above the energies considered here.) Although the fluorescence spectrum of the NpOH·H_2O complex when excited at the $S_1 \leftarrow S_0$ origin is sparse, moderately strong bands are observed at 467, 528, 713, and 1389 cm^{-1} shifts from the excitation. Of these, ion dips of more than 50% were observed only for the 713 (65 ± 5%) and 1390 (>80%) cm^{-1} bands. Depletions of 50 ± 5% were observed for the 528 and 467 cm^{-1} bands. This shows that IVR in the electronic ground state does not become significant until no less than 528 and no more than 713 cm^{-1} above the vibrationless level. This should be contrasted to the IVR onset in the S_1 at 400 cm^{-1}, a difference of at least 128 cm^{-1}, or 33%.

Although there are apparent differences in the observed S_0 and S_1 IVR thresholds, it should be noted that the fluorescence and ion-dip experiments probe somewhat different time scales. Fluorescence is usually integrated over several emission lifetimes, or more than 100 ns in this case ($\tau = 47$ ns at the origin). Ion dip takes place during the laser pulses, or in less than 5 ns. This means that slower processes may contribute more to the fluorescence experiment than to ion-dip spectra, possibly leading to a lower observed IVR threshold. To partially compensate for this, we have observed fluorescence from the +400 and +403 cm^{-1} levels with a time resolution of 30 ns. No difference in the spectra at short versus long times was observed. This narrows the range of IVR time scales probed by fluorescence, suggesting that the differences in S_0 and S_1 thresholds may be genuine.

Since intermolecular anharmonicity appears to be a crucial aspect of IVR in this complex, mode-specific differences in S_0 IVR can also be expected, as were found in the S_1. Unfortunately, there is only one intermolecular mode accessible in excitation, at 57 cm^{-1} above the origin. When ion-dip spectroscopy is performed via this level, the resulting dip spectrum is initially unremarkable. In contrast with the phenol·H_2O results,[26,29] few extra lines are observed, and they are weak. The strong lines are the same as when pumping the origin transition. However, the dip depths observed in this case are *not* the same as when pumping at the origin. The 467 cm^{-1} band can now be depleted to 65 ± 5%, indicating IVR activity. The 713 cm^{-1} transition shows a depletion of 70 ± 5%, or stronger IVR than before. It should be recalled that in these cases the dump transition is to a ground-state combination in which one quantum of the pumped intermolecular mode is excited. This quantum of excitation is apparently effective in enhancing IVR.

Conclusions

Resonant two-photon ionization and fluorescence spectra of the 1-naphthol·water hydrogen-bonded complexes are reported and interpreted with emphasis on intra-complex vibrational-energy redistribution and vibronic coupling.

In the R2PI absorption spectrum, intermolecular modes are extremely weak compared to other similar complexes. Only one intermolecular mode of 57 cm^{-1} is active in the spectrum. The ab initio results give no indication of any structural anomalies that might account for this. More structure is present in the R2PI spectrum of the deuterated species but could not be readily assigned.

Vibrational-energy redistribution in the S_1 is generally remarkably efficient through the noncovalent hydrogen bond. At excitation energies 400 cm^{-1} or higher above the $S_1 \leftarrow S_0$ origin, the fluorescence spectra change from a simple 1-naphthol-like pattern to a complex mixture of bands assignable to both relaxed and unrelaxed vibrations. This is attributed, by analogy to rigid molecules, to intermediate vibrational-energy redistribution, changing to dissipative IVR at about 834 cm^{-1} excess energy.

Both enhanced and suppressed IVR were observed for certain levels. In the pair of nearly degenerate levels at +400 and +403 cm^{-1}, there is a dramatic difference in IVR efficiency. The +400 cm^{-1} level undergoes nearly dissipative IVR, although this is otherwise not seen until much higher excess energy. The +403 cm^{-1} level is a clear intermediate IVR case, showing strong unrelaxed emission. The +553 cm^{-1} S_1 level is also a nearly "frozen" mode, exhibiting strong unrelaxed emission, although levels above and below show more extensive IVR. By use of lowest-order anharmonic coupling and the ab initio vibrational analysis of the complex, possible IVR-active "bath" levels for intermediate IVR were identified.

The exceptionally strong vibronic S_1-S_2 coupling observed in free naphthol for the 410/414 cm^{-1} pair was found to be partially inhibited by complexation with one water molecule. The details of the coupling are, however, very sensitive to the mass of the complexing molecule, since much stronger coupling was observed in the naphthol-OD·D_2O complex. This is apparently due to changes in the nature of the active vibrations due to harmonic-mode mixing. The high sensitivity of vibronic coupling to small changes in the solvent environment is also illustrated by the increased apparent vibronic activity of the +293 cm^{-1} level in the complex.

Electronic-state dependence of IVR was studied. The IVR threshold in the ground state was bracketed by ion-dip spectroscopy. When the $S_1 \leftarrow S_0$ origin was pumped, the apparent IVR onset in the S_0 was found to be ≥128 cm^{-1} higher than in the S_1. Pumping one quantum of the spectrally active 57 cm^{-1} intermolecular β_1 bend enhances S_0 IVR significantly.

Acknowledgment. R.K. and V.K. thank the ETH Zürich and Professor R. Zenobi for support. C.L., S.G., and S.L. thank the Schweizerische Nationalfonds for support, Project No. 20-47215.96.

References and Notes

(1) Förster, T. *Z. Elektrochem. Angew. Phys. Chem.* **1950**, *54*, 42.
(2) Weller, A. *Z. Elektrochem.* **1952**, *50*, 662.
(3) Hercules, D. M.; Rogers, L. B. *Spectrochim. Acta* **1959**, *15*, 393.
(4) Tramer, A.; Zaborowska, M. *Acta Phys. Pol.* **1968**, *34*, 821.
(5) Cheshnovsky, O.; Leutwyler, S. *Chem. Phys. Lett.* **1985**, *121*, 1.
(6) Lee, J.; Robinson, G. W.; Webb, S. P.; Philips, L. A.; Clark, V. *J. Am. Chem. Soc.* **1986**, *108*, 6538.
(7) Cheshnovsky, O.; Leutwyler, S. *J. Chem. Phys.* **1988**, *88*, 4127
(8) Knochenmuss, R.; Cheshnovsky, O.; Leutwyler, S. *Chem. Phys. Lett.* **1988**, *144*, 317.
(9) Knochenmuss, R.; Leutwyler, S. *J. Chem. Phys.* **1989**, *92*, 1268.
(10) Droz, T.; Knochenmuss, R.; Leutwyler, S. *J. Chem. Phys.* **1990**, *93*, 4520.
(11) Kim, S. K.; Li, S.; Bernstein, E. R. *J. Chem. Phys.* **1991**, *95*, 3119.
(12) Knochenmuss, R.; Holtom, G.; Ray, D. *Chem. Phys. Lett.* **1993**, *215*, 188.
(13) Knochenmuss, R.; Smith, D. E. *J. Chem. Phys.* **1994**, *101*, 7327.
(14) Kim, S. K. Wang, J.-K.; Zewail, A. H. *Chem. Phys. Lett.* **1994**, *228*, 369.
(15) Knochenmuss, R. *J. Chim. Phys.* **1995**, *92*, 445.
(16) Knochenmuss, R.; Muiño, P.; Wickleder, C. *J. Phys. Chem.* **1996**, *100*, 11218.
(17) Tubergen, M. J.; Levy, D. H. *J. Phys. Chem.* **1991**, *95*, 2175.
(18) Abe, H.; Mikami, H.; Ito, M. *J. Phys. Chem.* **1982**, *86*, 1768.
(19) Oikawa, A.; Abe, H.; Mikami, N.; Ito, M. *J. Phys. Chem.* **1983**, *87*, 5083.
(20) Fuke, K.; Kaya, K. *Chem. Phys. Lett.* **1983**, *94*, 97.
(21) Fuke, K.; Yoshiuchi, H.; Kaya, K.; Achiba, Y.; Sato, K.; Kimura, K. *Chem. Phys. Lett.* **1984**, *108*, 179.
(22) Lipert, R. J.; Bermudez, G.; Colson, S. D. *J. Phys. Chem.* **1988**, *92*, 3801.
(23) Lipert, R. J.; Colson, S. D. *J. Phys. Chem.* **1990**, *94*, 2358.
(24) Ebata, T.; Furukawa, M.; Suzuki, T.; Ito, M. *J. Opt. Soc. Am. B* **1990**, *7*, 1890.
(25) Ito, M.; Suzuki, T.; Furukawa, M.; Ebata, T. In *Dynamics of Polyatomic Van der Waals Complexes*; Halberstadt, N., Janda, K. C., Eds.; Plenum Press: New York, 1990; p 267.
(26) Stanley, R. J.; Castleman, A. W. *J. Chem. Phys.* **1991**, *94*, 7744.
(27) Schütz, M.; Bürgi, T.; Leutwyler, S. *THEOCHEM* **1992**, *276*, 117.
(28) Schütz, M.; Bürgi, T.; Leutwyler, S.; Fischer, S. *J. Chem. Phys.* **1993**, *98*, 3763.
(29) Stanley, R. J.; Castleman, A. W. *J. Chem. Phys.* **1993**, *98*, 796.
(30) Lipert, R. J.; Colson, S. D. *J. Chem. Phys.* **1993**, *89*, 4579.
(31) Dopfer, O.; Müller-Detlefs, K. *J. Chem. Phys.* **1994**, *101*, 8508.
(32) Ebata, T.; Mizuochi, N.; Watanabe, T.; Mikami, N. *J. Phys. Chem.* **1996**, *100*, 546.
(33) Schütz, M.; Bürgi, T.; Leutwyler, S.; Fischer, T. *J. Chem. Phys.* **1993**, *99*, 1469.
(34) Lakshminarayan, C.; Knee, J. L. *J. Phys. Chem.* **1990**, *94*, 2637.
(35) Syage, J. A. *J. Phys. Chem.* **1995**, *99*, 5772.
(36) Kim, S. K.; Wang, J.-K.; Zewail, A. H. *Chem. Phys. Lett.* **1994**, *228*, 369.
(37) Kim, S. K.; Li, S.; Bernstein, E. R. *J. Chem. Phys.* **1991**, *95*, 3119.
(38) Hineman, M. F.; Kelley, D. F.; Bernstein, E. R. *J. Chem. Phys.* **1993**, *99*, 4533.
(39) Kim, S. K.; Breen, J. J.; Willberg, D. M.; Peng, L. W.; Heikal, A.; Syage, J. A.; Zewail, A. H. *J. Phys. Chem.* **1995**, *99*, 7421.
(40) Demmer, D. R.; Leach, G. W.; Wallace, S. C. *J. Phys. Chem.* **1994**, *98*, 12834.
(41) Hopkins, J. B.; Powers, D. E.; Smalley, R. E. *J. Chem. Phys.* **1980**, *72*, 5039.
(42) Hopkins, J. B.; Powers, D. E.; Mukamel, S.; Smalley, R. E. *J. Chem. Phys.* **1980**, *72*, 5049.
(43) Hopkins, J. B.; Powers, D. E.; Smalley, R. E. *J. Chem. Phys.* **1981**, *74*, 5971.
(44) Gruner, D.; Brumer, P. *J. Chem. Phys.* **1991**, *94*, 2848. Gruner, D.; Brumer, P. *J. Chem. Phys.* **1991**, *94*, 2862.
(45) McIlroy, A.; Nesbitt, D. J. In *Advances in Molecular Vibrations and Collision Dynamics 1A*; Bowman, J. M., Ed., JAI Press: Greenwich, 1991; p 109. Lehmann, K. K.; Scoles, G.; Pate, B. H. *Annu. Rev. Phys. Chem.* **1994**, *45*, 241.
(46) Topp, M. R. Fast relaxation in jet-cooled van der Waals clusters involving large aromatic molecules. In *Jet Spectroscopy and Molecular Dynamics*; Hollas, J. M., Phillips, D., Eds.; Blackie Academic and Professional: London, 1995; p 309. Smith, P. G.; Topp, M. R. *Chem. Phys. Lett* **1994**, *229*, 21.
(47) Kunst, A. G. M.; Rettschnick, R. P. H In *Dynamics of Polyatomic Van Der Waals Complexes*; Halberstadt, N., Janda, K. C., Eds.; Plenum Press: New York, 1990; p 277.
(48) Felker, P. M.; Zewail, A. H. Ultrafast dynamics of IVR in molecules and reactions. In *Jet Spectroscopy and Molecular Dynamics*; Hollas, J. M., Phillips, D., Eds.; Blackie Academic and Professional: London, 1995; p 222.
(49) Bernstein, E. R. *Dynamics of Polyatomic Van der Waals Complexes*; Halberstadt, N., Janda, K. C., Eds; Plenum Press: New York, 1990; p 295.
(50) Bernstein, E. R. *Ann Rev. Phys. Chem.* **1995**, *46*, 197.
(51) Stephenson, T. A.; Rice, S. A. *J. Chem. Phys.* **1984**, *81*, 1083.
(52) Weber, P. M.; Rice, S. A. *J. Phys. Chem.* **1988**, *92*, 5470.
(53) Weber, P. M.; Rice, S. A. *J. Chem. Phys.* **1988**, *88*, 6107, 6120.
(54) Brumbaugh, D. V.; Kenny, J. E.; Levy, F. H. *J. Chem. Phys.* **1983**, *78*, 3415.
(55) Butz, K. W.; Catlett, D. L., Jr.; Ewing, G. E.; Krajnovich, D.; Parmenter, C. S. *J. Phys. Chem.* **1986**, *90*, 3533.
(56) Oh, H.-K.; Parmenter, C. S.; Su, M.-C. *Ber. Bunsen-Ges. Phys. Chem.*. **1988**, *92*, 253.
(57) Gilbert, B. D.; Parmenter, C. S.; Oh, H.-K. *J. Phys. Chem.* **1995**, *99*, 2444.
(58) Zhang, X.; Knee, J. L. *Faraday Discuss.* **1994**, *97*, 299. Smith, J. M.; Zhang, X.; Knee, J. L. *J. Phys. Chem.* **1995**, *99*, 1768.
(59) Sinclair, W. E.; Pratt, D. W. *J. Chem. Phys.* **1996**, *105*, 7942.
(60) Riedle, E.; Sussmann, R.; Weber, T.; Neusser, H. J. *J. Chem. Phys.* **1996**, *104*, 865.
(61) Abou-Zied, O. K.; Demmer, D. R. M.; Wallace, S. C.; Steer, R. P. *Chem. Phys. Lett.* **1997**, *266*, 75.
(62) Quack, M. *Annu. Rev. Phys. Chem.* **1990**, *41*, 6120.
(63) Beil, A.; Luckhaus, D.; Quack, M.; Stohner, J. *Ber. Bunsen-Ges. Phys. Chem.* **1997**, *101*, 311
(64) Hopkins, J. B.; Langridge-Smith, P. R. R.; Smalley, R. E. *J. Chem. Phys.* **1983**, *78*, 3410.
(65) Suzuki, T.; Mikami, N.; Ito, M. *J. Phys. Chem.* **1986**, *90*, 6431.
(66) Frisch, M. J.; Trucks, G. W.; Schlegel, H. B.; Gill, P. M. W.; Johnson, B. G.; Wong, M. W.; Foresman, J. B.; Robb, M. A.; Head-Gordon, M.; Replogle, E. S.; Gomperts, R.; Andres, J. L.; Raghavachari, K.; Binkley, J. S.; Gonzalez, C.; Martin, R. L.; Fox, D. J.; Defrees, D. J.; Baker, J.; Stewart, J. J. P.; Pople, J. A. *Gaussian 92/DFT*, Revision G.1; Gaussian, Inc.: Pittsburgh, PA, 1993.
(67) Felker, P. M.; Zewail, A. H. *J. Chem. Phys.* **1984**, *82*, 2975.
(68) Beyer, T.; Swinehart, D. R. *ACM Commun.* **1973**, *16*, 379.
(69) Parmenter, C. S. *Faraday Discuss. Chem. Soc.* **1983**, *75*, 7.
(70) Humphrey, S. J.; Pratt, D. W. *Chem. Phys. Lett.* **1996**, *257*, 169.
(71) Felker, P. M.; Zewail, A. H. *J. Chem. Phys.* **1983**, *78*, 5266.
(72) Gruner, D.; Nguyen, A.; Brumer, P. *J. Chem. Phys.* **1994**, *101*, 10366.
(73) Nesbitt, D. J.; Field, R. W. *J. Phys. Chem.* **1996**, *100*, 12735.
(74) Small, G. J. *J. Chem. Phys.* **1971**, *54*, 3300.
(75) Orr, G.; Small, G. J. *Chem. Phys. Lett.* **1973**, *21*, 93.
(76) Takahashi, J.; Shida, T. *Bull. Chem. Soc. Jpn.* **1994**, *67*, 2038.
(77) Wategaonkar, S.; Doraiswamy, S. *J. Chem. Phys.* **1997**, *106*, 4899.
(78) Bürgi, T.; Droz, T.; Leutwyler, S. *Chem. Phys. Lett.* **1995**, *246*, 291.